

PAPER

CrossMark
click for updatesCite this: *J. Mater. Chem. A*, 2016, 4, 1991

Photo-induced degradation of lead halide perovskite solar cells caused by the hole transport layer/metal electrode interface

Dong Wei,^a Tianyue Wang,^a Jun Ji,^a Meicheng Li,^{*ab} Peng Cui,^a Yaoyao Li,^a Guanying Li,^a Joseph Michel Mbengue^a and Dandan Song^a

Lead halide perovskite solar cells (PSCs) suffer from poor long-term stability, especially due to photo-induced degradation, as PSCs function under continuous sunlight. However, the origins of this instability have not been clearly explored. Herein, the photo-induced degradation of PSCs with mesoporous and planar architectures are investigated, respectively, and the main origin is proved to be correlated with the hole transport material (HTM)/metal (Au) electrode interface. The solar irradiation of PSCs causes significant deterioration of device performance, with the efficiency decreasing from approximately 18% to 2.46% for planar PSCs in 180 min. Electrical analysis of the PSCs and XPS measurements show that the deteriorated performance is induced by retarded carrier extraction from the HTM to the Au electrode, due to a broken interface binding. Accordingly, *in situ* renewal of the Au electrode was found to cause notable recovery (approximately 80%) of the device performance of both mesoporous and planar PSCs. In comparison, the material degradation of perovskite and the TiO₂/perovskite interface were also studied; however, these showed minor effects on the photo-induced degradation of PSCs. These results indicate that the photo-induced degradation of PSCs is mainly caused by the HTM/Au interface. This study provides an important insight into the photo-induced degradation of PSCs, and is crucial for the fabrication of highly photo-stable PSCs.

Received 27th October 2015
Accepted 31st December 2015

DOI: 10.1039/c5ta08622a

www.rsc.org/MaterialsA

Introduction

Lead halide perovskite (MAPbX₃, MA = CH₃NH₃, X = I, Cl, Br) materials and devices have enabled tremendous improvements in the application of solar cells as active materials, especially for their power conversion efficiency, which has increased from 3.8% to 20.1% over the last 5 years.^{1–6} This rapid progress suggests that perovskite solar cells (PSCs) possess extraordinary potential to replace traditional silicon solar cells, due to their large absorption coefficients and high carrier mobilities.^{7,8} Along with the rapid increase of device efficiency, PSCs also face great challenges in terms of long-term stability.^{9,10} Perovskites have been shown to decompose in many circumstances,^{11–14} especially in moist atmosphere, leading to decreased photo-voltaic performance of their related PSCs. Moreover, photo-induced degradation is also obvious in PSCs,^{15–18} and it causes the photovoltaic performance of PSCs to worsen with prolonged irradiation time. Compared to degradation by moisture, which can be readily prevented by encapsulating the device, photo-

induced degradation under solar irradiation is a greater problem, because PSCs always operate under irradiation; however, the related degradation process and its mechanisms have not been well investigated.

The degradation induced by irradiation has been proposed to be caused by several factors in previous studies. The earliest studies ascribed this degradation to UV light-induced instability *via* TiO₂ as the mesoporous layer of mesoporous PSCs; this can be reduced to some extent by replacing TiO₂ with Al₂O₃ as the mesoporous layer or by filtering UV light during irradiation.^{15,18} However, PSCs containing Al₂O₃ still exhibit obvious degradation under light irradiation, implying that other degradation mechanisms exist in PSCs. Some other studies attribute the degradation under irradiation to decomposition of the perovskites.¹⁷ Therefore, a study was performed on individual perovskite films; however, the study showed that integrated irradiation (100 suns for 60 min, equalling 1 sun for 100 h) of perovskite films does not cause this decomposition, except at evaluated temperatures.¹⁴ Therefore, degradation under irradiation at room temperature is probably not caused by decomposition of the perovskites. From these investigations, it can be observed that the mechanism of photo-degradation in PSCs is still not clear, and urgently remains to be explored.

In this context, the photo-induced degradation of PSCs and its mechanism are investigated. Significant decay in the

^aState Key Laboratory of Alternate Electrical Power System with Renewable Energy Sources, School of Renewable Energy, North China Electric Power University, Beijing 102206, China. E-mail: mcli@ncepu.edu.cn; Fax: +86 10 6177 2951; Tel: +86 10 6177 2951

^bChongqing Materials Research Institute, Chongqing 400707, China

photocurrents and efficiency of PSCs with both mesoporous and planar architectures are observed under continuous irradiation, and a novel degradation mechanism driving this photo-induced deterioration, correlated with the hole transport material (HTM)/metal electrode interface, is proposed. The electrical and chemical changes in the characteristics of the interface after irradiation are proved to be the main reasons for photo-induced degradation. Furthermore, it is shown that *in situ* refreshing of the metal electrode could eliminate the photo-induced degradation of PSCs to a great extent.

Experimental

Fabrication of $\text{CH}_3\text{NH}_3\text{PbI}_3$ films and PSCs

$\text{CH}_3\text{NH}_3\text{PbI}_3$ films were fabricated using a modified sequential deposition process.^{19,20} PbI_2 was firstly loaded by spin-coating onto a compact TiO_2 layer (planar architecture) or a scaffold TiO_2 layer (mesoporous architecture), and then dipped into a solution of $\text{CH}_3\text{NH}_3\text{I}$ in ultra-dry isopropanol for 5 min; this was followed by formation of the $\text{CH}_3\text{NH}_3\text{PbI}_3$ films by annealing at 150 °C. All the procedures were carried out in a glove box filled with high purity N_2 . For the planar structure, a compact TiO_2 layer was fabricated on FTO by TiCl_4 treatment. For the mesoporous structure, a compact TiO_2 layer and a scaffold TiO_2 layer were spin-coated in sequence, then annealed at 500 °C for 30 min.²¹ The HTM layer was obtained by spin-coating 2,2',7,7'-tetrakis[*N,N*-di(4-methoxyphenyl)amino]-9,9'-spirobifluorene (spiro-MeOTAD) solution (dissolved in chlorobenzene) with standard additives, including *tert*-butylpyridine and lithium bis(trifluoromethanesulfonyl) imide in a glove box, followed by oxidation in clean air for 4 h. Subsequently, the Au electrode was applied by sputtering.

Characterization and simulation

Current–voltage curves were measured using a source meter (Keithley 2400) under AM 1.5G irradiation with a power density of 100 mW cm^{-2} from a solar simulator (XES-301S + EL-100). KPFM was carried out using an Agilent SPM 5500 microscope and measured in the tapping mode. Device simulation was carried out using wxAMPS software, based on the planar architecture of an FTO/compact TiO_2 (30 nm)/perovskite (350 nm)/HTM (150 nm)/Au electrode.

Results and discussion

The photo-induced degradation of mesoporous PSCs has been studied in previous reports,^{15–18} whereas for planar PSCs, detailed investigation is scarce; therefore, herein, the photo-induced degradation of PSCs with both architectures are investigated. The schematic of the PSCs with planar or mesoporous architectures are shown in Fig. 1a. The light irradiates from the FTO/glass side and is absorbed by the perovskite film. The residual light travels across the organic HTM and is reflected by the metal (typically Au) electrode to the perovskite film for secondary absorption. Therefore, the degradation caused by irradiated light may occur at any of the components

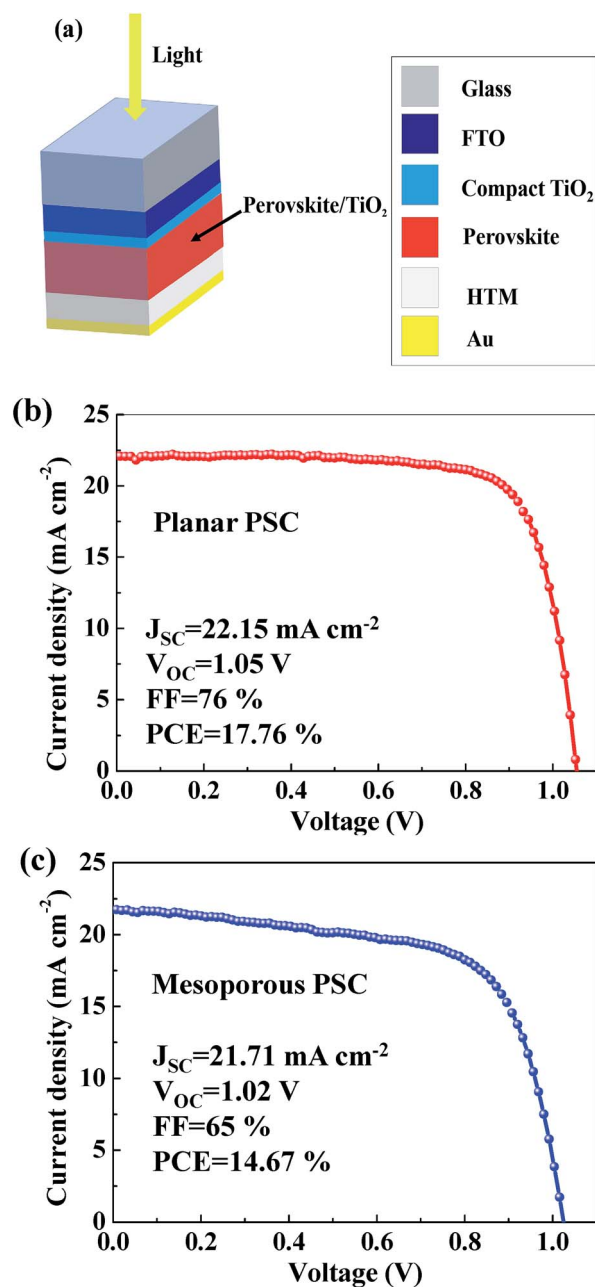


Fig. 1 (a) Schematic of typical PSCs with planar and mesoporous architectures. (b and c) Best-performance J – V curves of (b) planar and (c) mesoporous PSC measured under an irradiation of 100 mW cm^{-2} with a scan rate of 150 mV s^{-1} .

in the PSCs. Fig. 1b shows the photocurrent–voltage (J – V) curve of the fresh, best-performing planar PSC, which yields a short circuit current (J_{sc}), an open circuit voltage (V_{oc}) and a fill factor (FF) of 22.15 mA cm^{-2} , 1.05 V, and 76%, respectively, and a final power conversion efficiency (PCE) of 17.76%. Fig. 1c presents the J – V curve of the fresh, best-performing mesoporous PSC, which shows a PCE of 14.67%. The average values of the photovoltaic parameters were also calculated for multiple identical PSCs and are listed in Table 1. The PCEs of the mesoporous PSCs are slightly lower than those of the planar PSCs,

Table 1 The photovoltaic parameters of PSCs with planar and mesoporous architectures^a

Solar cells		J_{SC} (mA cm ⁻²)	V_{OC} (V)	FF (%)	PCE (%)
Planar	Best	22.15	1.05	76	17.76
	Average	21.51 ± 0.77	1.05 ± 0.01	72 ± 2	16.39 ± 0.74
Mesoporous	Best	21.71	1.02	65	14.67
	Average	21.29 ± 0.45	1.02 ± 0.01	64 ± 1	14.21 ± 0.45

^a The best values are obtained from the PSC with the highest PCE. The average values and the standard deviations are obtained from ten identical solar cells.

which is mainly caused by the relatively low FF. In addition to the different fabrication methods for these two types of PSCs, their efficiency difference is probably induced by the relatively low conductivity of the TiO₂ layer compared to that of the perovskite layer.²²

With continuous irradiation, *i.e.*, under the actual working conditions of solar cells, the PSCs were observed to degrade, as shown in Fig. 2a–d. With the irradiation time from 0 to 180 min, it is clear that all the photovoltaic parameters, especially J_{SC} and FF, decrease with increasing time. As a result, the PCE decreases by more than 80% of its initial value. These decreases can be partially recovered by placing the PSC in the dark for a period of 90 min. The recovery of the photovoltaic parameters by storing in the dark corresponds to the reversible changes of the PSC under irradiation. However, most of the photo-induced degradation is irreversible, leading to degraded performance of the PSCs. As the PSCs were measured in ambient air, it was speculated that the degradation derives from the moisture effect rather than photo-induced degradation. Therefore, a series of PSCs, which were placed in the same ambient air but stored in the dark instead of under continuous irradiation, were monitored. As shown in Fig. 2a–d, the PSC without continuous irradiation shows little degradation, proving the stability of PSCs in

ambient air. Therefore, the degradation of the PSCs under irradiation is indeed caused by irradiation rather than by moisture in ambient air.

Photo-induced degradation does not solely occur in planar PSCs, but also in mesoporous PSCs. As shown in Fig. 3, all the photovoltaic parameters, including J_{SC} , V_{OC} , FF and PCE, of the mesoporous PSCs decrease with increasing irradiation time; these results are consistent with those for the planar PSCs. Among these parameters, J_{SC} and FF also decrease more obviously than V_{OC} , which is in accordance with the results for the planar PSCs. Therefore, the photo-induced degradation of PSCs is a common and fundamental phenomenon in both types of PSCs, which arouses our interest in exploring the intrinsic mechanisms. The degradation magnitude is less in mesoporous PSCs than in planar PSCs. For example, after irradiation for 90 min, the PCE of a mesoporous PSC retains over 60% of its initial value, whereas the PCE of a planar PSC decreases to 20% of its initial value. This difference caused by the architecture of the PSCs is not induced by the different initial efficiency values, as it is found that the planar PSCs with different initial efficiencies (14.7% to 17.7%) show similar degrees of degradation in device efficiency. The difference is correlated with the photo-induced degradation mechanism, which will be discussed later.

To obtain insight into the mechanism of the photo-induced degradation, the UV-Vis absorption spectra of the perovskite films were characterized to test if the perovskite films

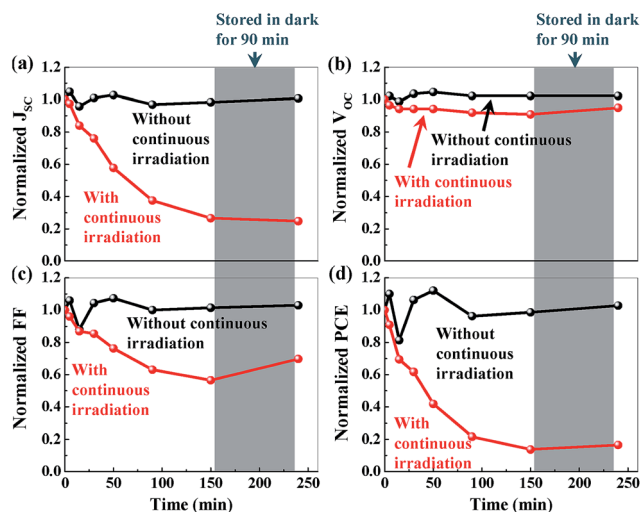


Fig. 2 Photovoltaic parameters of the planar PSCs without encapsulation with and without irradiation as a function of irradiation time in ambient air (50% to 60% humidity at room temperature). (a) Normalized J_{SC} . (b) Normalized V_{OC} . (c) Normalized FF. (d) Normalized PCE.

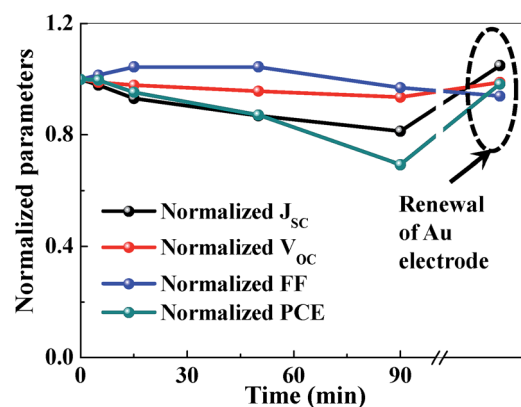


Fig. 3 Photovoltaic parameters of mesoporous PSCs without encapsulation as a function of irradiation time in ambient air (50% to 60% humidity at room temperature). The renewal of the Au electrode was carried out by removal of the irradiated Au electrode and subsequent deposition of the new one.

decompose upon irradiation. As shown in Fig. 4a, the absorption spectra of the fresh and the degraded perovskite films both exhibit typical absorption character of the absorption band-edge at 1.63 eV. The absorption intensity is lower in irradiated perovskite films, demonstrating the degradation of the

perovskite films. However, the degradation degree of the absorption intensity (about 20% at 500 nm) is much lower than that of the J_{SC} (80%). As the generation of photocurrent correlates with the light harvesting efficiency of the perovskite, which is determined by the absorption intensity of the perovskite; therefore, it is speculated that the degradation of the absorption intensity is not the main origin of the degraded J_{SC} and device performance of the PSCs. The digital images of the PSCs before and after degradation (Fig. 4a insets) also demonstrate that the perovskite films show little change in appearance after irradiation. Moreover, the morphologies of the perovskite films and the devices present minor changes with irradiation, as shown in Fig. 4b and c, respectively. X-ray diffraction spectra of the fresh (without irradiation) and photo-degraded (with irradiation) PSCs without Au electrodes are presented in Fig. 4d. The XRD patterns of both the fresh and degraded PSCs can be indexed to the diffraction peaks of perovskite and FTO, revealing no change in the crystal structure of the perovskite during irradiation. No diffraction peaks from PbI_2 , typically represented by an intense peak located at 14.2° , can be observed. Moreover, no diffraction peaks from perovskite hydrate²³ are observed. These observations reveal that the photo-induced degradation of the PSCs is not similar to moisture-induced degradation, as the latter is typically correlated with the decomposition of perovskite to PbI_2 or perovskite hydrate. Therefore, the photo-induced degradation of the PSCs is not mainly caused by the change in the perovskite films, but can be correlated with other parts of the PSCs.

The photo-induced degradation of mesoporous PSCs has previously been ascribed to UV-induced degradation of the TiO_2 in the mesoporous layer.¹⁵ Our results show that the planar PSCs with smaller TiO_2 /perovskite interfaces (no mesoporous TiO_2 layer) yield more severe degradation; this suggests that this interface is probably not the main origin of this degradation in the as-fabricated PSCs. Considering the good material stability of the materials utilized in PSCs, including TiO_2 and spiro-OMeTAD (HTM), which are widely used in other types of solar cells,^{24–26} the degradation thus may occur at the perovskite/HTM or HTM/Au interfaces. To check the change in the HTM/Au interface, the Au electrode was renewed by removing it from the degraded PSC and depositing a new one. The removal of the Au electrode was carried out by a tape peeling method with Scotch tape, which can perfectly remove the Au electrode from the organic HTM due to the weak bonding between metal and organic materials.²⁷ Subsequently, a fresh Au electrode was deposited on the degraded stacks to create a fresh HTM/Au interface. Interestingly, the performance of the mesoporous PSC with the new Au electrode recovered significantly. As shown in Fig. 3, the PCE of the degraded PSC with the renewed Au electrode is 14.42%, which reaches 98.29% of the PCE of the fresh PSC.

The planar PSCs also exhibited significant recovery in photovoltaic performance after the Au electrode was refreshed, as shown in Fig. 5a, demonstrating that the photo-induced degradation mainly occurs at the HTM/Au interface. As can be observed from Fig. 5a, the photo-induced degradation decreases the PCE of the PSC more than 80%, from 17.76% to

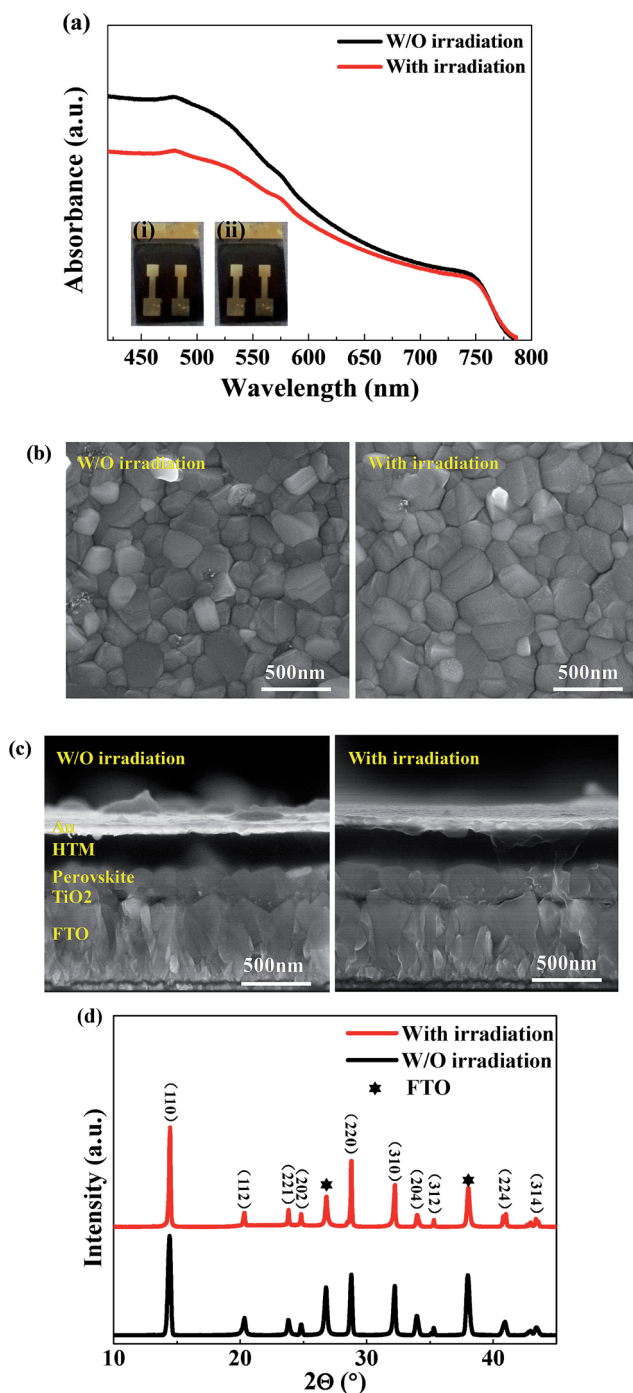


Fig. 4 (a) UV-Vis absorption spectra of perovskite film before and after irradiation. Insets in the UV-Vis absorption spectra (a) show digital images of the planar PSCs before irradiation (i) and after irradiation (ii). (b and c) Scanning electron microscopy (SEM) images of the perovskite films (b) and the PSCs (c). (d) XRD spectra of the PSCs after removing the Au electrode.

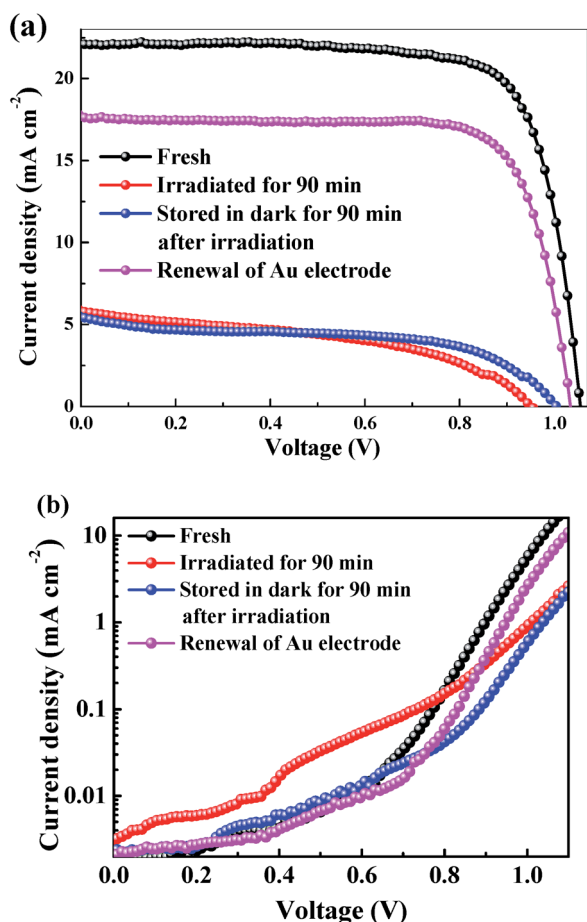


Fig. 5 (a) Photo J - V curves and (b) dark J - V curves of fresh and degraded planar PSCs. The renewal of the Au electrode was carried out by removal of the irradiated Au electrode and subsequent deposition of a new electrode.

2.46%. After storage in the dark for 90 min, the PCE recovered slightly to 2.95%. In contrast, the PCE was obviously recovered through refreshing the Au electrode by close to 80%, reaching 13.99%. Therefore, the photo-induced degradation mainly occurs at the HTM/Au electrode interface. As the photo-induced degradation at this interface depends on the light traveling through the PSCs, the mesoporous PSCs, which are thicker (~ 600 nm for the mesoporous layer and the perovskite capping layer), with less light reaching the HTM/Au interface, show less degradation than the planar PSCs, which have a thinner perovskite layer (~ 350 nm). The unrecovered degradation of the PSCs by renewal of the Au electrode is caused by the partially recovered J_{SC} , due to the degradation of the perovskite film with low absorption intensity.

To study the change in the HTM/Au electrode interface and its correlation with the device performance, the electrical parameters, including the series resistance (R_s), the shunt resistance (R_{sh}), the reverse saturation current (J_0) and the diode ideality factor (m) of the solar cells without degradation (fresh), irradiated for 90 min, stored in the dark for 90 min after irradiation and recovered by renewal of the Au electrode, were

calculated by fitting J - V curves (shown in Fig. 5a) with the equation as follows:

$$J = J_{SC} - J_0 \left[\exp \frac{-q(V + AJR_s)}{mk_B T} - 1 \right] - \frac{V + AJR_s}{AR_{sh}}$$

where A and m represent the device area and the diode ideality factor, respectively. The calculated values are listed in Table 2. It is clear that all the electrical parameters are diminished in the PSCs that were irradiated for 90 min. Increased R_s reflects increased bulk resistance, leading to lowered J_{SC} and FF for the irradiated PSCs. R_{sh} is sufficiently large for both the degraded and fresh PSCs; thus, they have similar V_{OC} values. J_0 correlates with carrier recombination in the p-region and n-region; therefore, the higher J_0 value for the irradiated PSC corresponds to higher carrier recombination in these regions than in those of the fresh PSC. After storage in dark for 90 min, R_s changed little, whereas J_0 was reduced to some extent. By refreshing the Au electrode, both R_s and J_0 were reduced, and were similar to those of fresh PSCs. Therefore, the degradation of the PSCs and their recovery by renewal of the Au electrode are caused by variations in R_s and J_0 , which cause the changes in J_{SC} , FF and the resultant PCE.

The dark J - V curves were characterized and are shown in Fig. 5b. The dark current at a low voltage scale reflects the carrier recombination in the space charge region of the PSCs (*i.e.*, the perovskite layer sandwiched between the TiO_2 and HTM layers), whereas the current after the threshold voltage is determined by the R_s of the PSCs. From the dark J - V curves, it is clear that carrier recombination in the space charge region is higher in the degraded PSCs and can be reduced by subsequent storage of the PSCs in the dark, corresponding to the reduced dark current of PSCs stored in the dark for 90 min. This implies that the photo-induced degradation occurs at regions other than the space charge region. However, R_s irreversibly increases after irradiation, according to the reduced dark current at the high voltage scale, and can only be decreased by renewal of the Au electrode. This indicates that the effect of the irradiation process on R_s mainly increases at the HTM/metal electrode interface and can be reduced with renewal of the HTM/Au interface. The increased R_s at the HTM/Au electrode interface with irradiation decreases hole transport from the HTM to the Au electrode, and thus increases the carrier recombination at this region, leading to the large J_0 in the irradiated PSCs.

To find out the influence of irradiation on the electrical properties of the HTM/Au interface, Kelvin probe force microscopy (KPFM) was employed to detect the electrical properties of HTM near the HTM/electrode interface. To detect this information at the interface, ultra-thin HTM films were deposited on Au and FTO electrodes followed by irradiation for 90 min. Topographic images of the HTM films on the Au electrodes before and after irradiation are shown in Fig. 6a and b. It is clear that the morphology and roughness of the HTM are changed only slightly after irradiation, apart from their possible effect on device performance. In the potential images shown in Fig. 6e and f, the surface potential of the HTM varies dramatically with irradiation (*i.e.*, the mean potential is lowered by 150 mV with irradiation). In comparison, HTM films on FTO

Table 2 Fitted electrical parameters of fresh and degraded PSCs

Solar cells	R_s (Ω)	R_{sh} ($k\Omega$)	J_0 (mA cm^{-2})	m	J_{sc} (mA cm^{-2})
Fresh	102.9	446	2.54×10^{-6}	2.54	22.15
Irradiated for 90 min	349.2	133	6.64×10^{-3}	5.51	5.89
Stored in the dark for 90 min	358.8	191	6.05×10^{-4}	4.47	5.51
Renewal of Au electrode	182.1	418	1.82×10^{-5}	2.89	17.79

(Fig. 6c, d, g and h) seem to be insensitive to sustained irradiation; they show similar morphologies and potentials (difference less than 50 mV). As the surface potential of the HTM is determined by the Fermi level of the HTM and the work function of the tip, a lowered potential corresponds to the loss of electrons or the gain of holes in the HTM. Considering the p-type feature of the HTM, the reduced potential can be ascribed to a gain of holes in the HTM. At the Au/HTM interface or the FTO/HTM interface, holes diffuse from the HTM to Au or FTO, establishing the thermal equilibrium of the carriers. Therefore, the reduced potential of the HTM on Au after irradiation indicates decreased hole diffusion from the HTM to Au. This is in accordance with the increased R_s , which decreases hole transport from the HTM to the Au electrode in the PSCs after irradiation. The minor change in the HTM on FTO reveals that the HTM itself shows little change by irradiation; moreover, the HTM/FTO interface is very stable to irradiation.

To study the effect of irradiation on the chemical properties of the HTM/Au interface, X-ray photoelectron spectroscopy (XPS) was employed to characterize the surface energy levels of the HTM/Au interface. Fig. 7a shows the survey spectra of ultrathin HTM films deposited on Au electrodes without

irradiation and with irradiation for 90 min. In addition to the peaks of C, N and F from the HTM, a group of peaks corresponding to Au 4f binding energies are also observed (Fig. 7a inset). This indicates that the HTM is thin enough to detect changes in the HTM/Au interface. By comparing the peak locations of the Au 4f spectra before and after irradiation, a shift of 1 eV to a lower binding energy is observed for the irradiated sample. The binding energy for Au 4f_{5/2} is 83.08 eV for the irradiated sample; this is close to that of elemental Au. The binding of Au with other elements typically causes a positive shift in its binding energy. Therefore, the higher binding energy of Au in the HTM/Au sample without irradiation implies the binding of Au with the atoms from the HTM; these bonds are broken by irradiation. The O1s spectra, as shown in Fig. 7b, reveals a positive shift of the binding energy from 531.6 eV to 532.1 eV for O 1s by irradiation. This trend is in accordance with the negative shift of the Au binding energy after irradiation, indicating chemical contact between Au/HTM though an Au–O bond, which is broken upon irradiation. These findings are similar to observations in organic light emitting diodes (OLEDs), in which metal electrode (Ag and Al)/organic material interfaces are also changed by light irradiation.^{27,28} It is worth

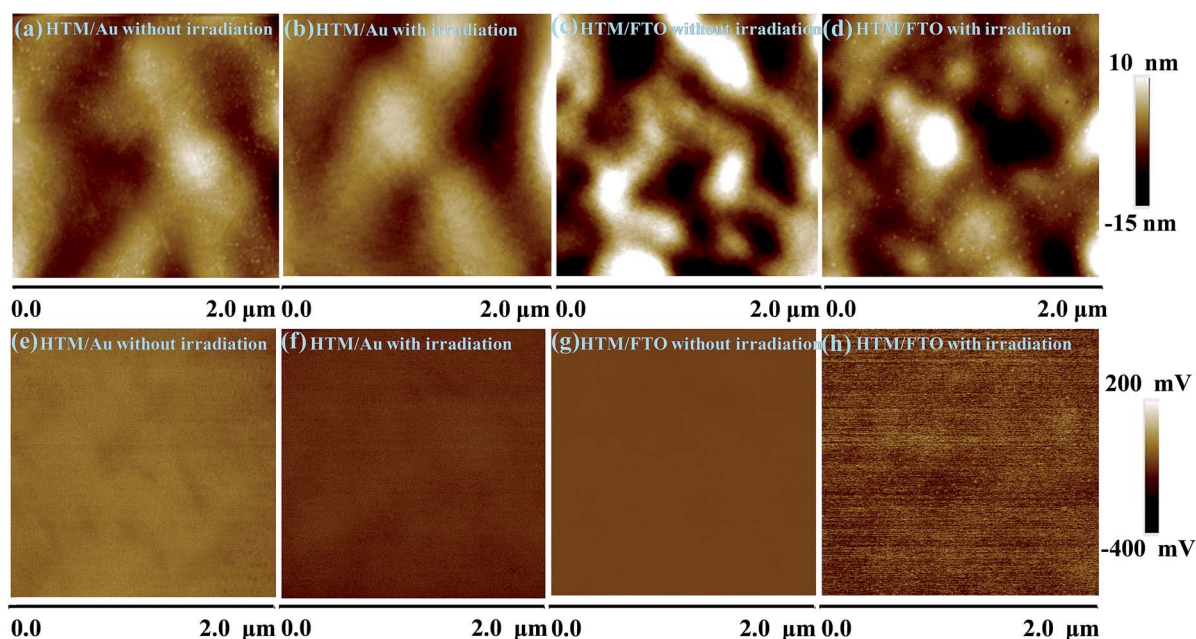


Fig. 6 Topography and potential images of ultrathin HTM films coated on Au and FTO glass, respectively. (a–d) The topography images and (e–h) the potential images from the HTM films without irradiation or irradiated for 90 min.

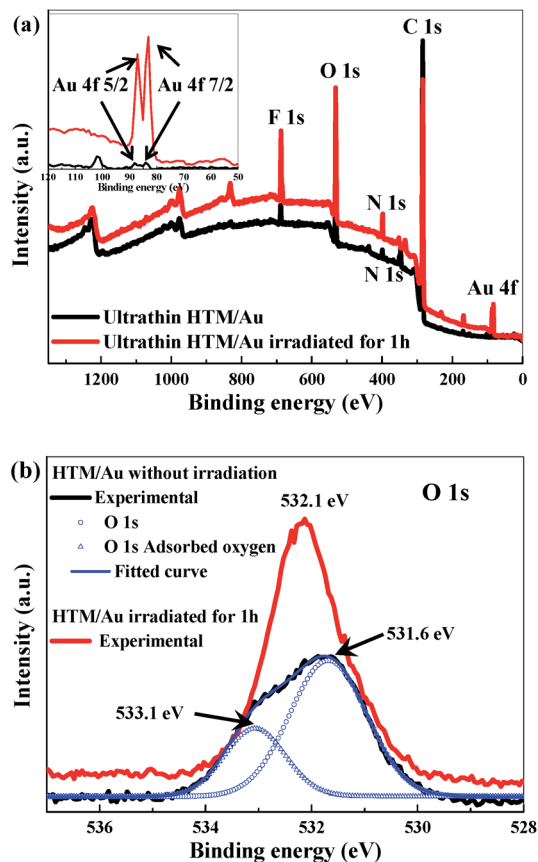


Fig. 7 (a) XPS spectra from HTM/Au stacks without or with irradiation for 1 h and the inset graph represents the peaks of Au 4f binding energies without and with irradiation. (b) O 1s electron binding energy spectra from the same samples. The O 1s curves were fitted by Gaussian fitting. The binding energy located at 533.1 eV derives from the adsorbed oxygen on the sample.

noting that the damaged HTM/Au interface does not correlate with the fabrication method of the Au electrode. In thermally evaporated Au electrodes (*i.e.*, the typically used method for depositing Au electrodes), the degradation of the PSCs is similar to that in the as-fabricated PSCs with sputtered Au electrodes (data is not shown here in the interest of saving space).

The damaged contact at the organic/metal interface under continuous irradiation decreases the surface potential due to shifts of the binding energy. Therefore, the surface potential measured by KPFM is lower after continuous irradiation. This low surface potential is expected to lead to insufficient hole extraction from the HTM to the Au electrode. To verify this effect, the variations of free hole density of the HTM surface (3 nm) with the surface potential of the HTM (the highest unoccupied molecular orbital, HOMO) in planar PSCs was simulated using wxAMPS,²⁹ which is reliable software to simulate thin film solar cells. As shown in Fig. 8, the surface HOMO level was adjusted from 5.12 eV to 5.32 eV to evaluate the surface potential change of the HTM. It can be observed that the free hole density at the HTM surface is deeply influenced by the surface HOMO level of the HTM, indicating that the surface potential of the HTM plays a critical role in the charge

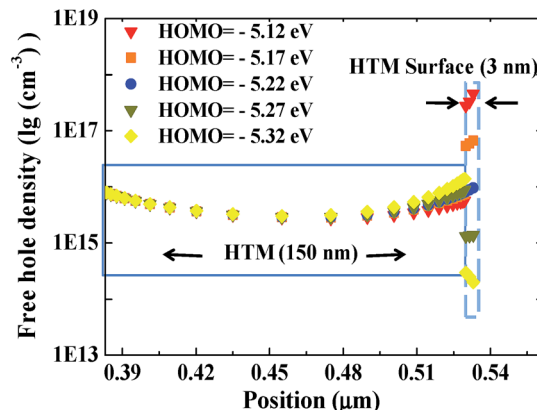


Fig. 8 Spatial distribution of free holes in the HTM of the planar PSCs. The surface HOMO level was adjusted from 5.12 eV to 5.32 eV to evaluate the surface potential change of the HTM. The HOMO level of the bulk HTM is 5.22 eV.

extraction. When the surface HOMO level shifts to the vacuum level by 50 meV, corresponding to a 50 mV increase in the surface potential, the free hole density at the HTM surface dramatically increases. In the degraded HTM, which corresponds to a low surface potential (a low HOMO level), fewer holes can be extracted to the HTM surface. Therefore, the carrier collection will be less efficient in the degraded HTM, which is in accordance with the experimental results.

On the basis of the abovementioned results, it is clear that the organic/metal interface plays a critical role in carrier collection, and thus is very important for the photo-stability of PSCs. Therefore, suitable materials that can improve the contact between the HTM and the Au electrode, such as LiF³⁰ and thiols,³¹ can enhance the stability of PSCs. In addition, the utilization of inorganic HTMs is also a solution for photo-induced degradation. Further exploration of methods to improve the organic HTM/Au electrode interface is crucial.

Conclusions

In conclusion, the photo-induced degradation of PSCs is proved to be caused by the organic HTM/Au electrode interface, which is a fundamental issue in PSCs with either mesoporous or planar architectures. In contrast, the degradation of the perovskite itself or other parts of the PSCs is minor. It is found that the chemical bonding between HTM and Au is deteriorated by continuous irradiation, causing insufficient hole extraction at this interface. Consequently, the series resistance and carrier recombination of the PSCs are increased, leading to their degraded photovoltaic performance. Renewal of the Au electrode can effectively recover the performance of the degraded PSCs with mesoporous and planar architectures. Moreover, suggestions for the elimination of photo-induced degradation are also proposed. These results provide a new photo-induced degradation mechanism beyond that ascribed to the presence of TiO₂ in mesoporous PSCs, and are important for developing photo-stable and highly efficient PSCs.

Acknowledgements

This study was supported partially by the National High-tech R&D Program of China (863 Program, No. 2015AA034601), the National Natural Science Foundation of China (Grant no. 91333122, 51402106, 51372082, 51172069, 61204064 and 51202067), Ph.D. Programs Foundation of Ministry of Education of China (Grant no. 20120036120006, 20130036110012), the Par-Eu Scholars Program, and the Fundamental Research Funds for the Central Universities.

References

- 1 K. Akihiro, T. Kenjiro, S. Yasuo and M. Tsutomu, *J. Am. Chem. Soc.*, 2009, **131**, 6050–6051.
- 2 J. H. Im, C. R. Lee, J. W. Lee, S. W. Park and N. G. Park, *Nanoscale*, 2011, **3**, 4088–4093.
- 3 H. S. Kim, C. R. Lee, J. H. Im, K. B. Lee, T. Moehl, A. Marchioro, S. J. Moon, R. Humphry-Baker, J. H. Yum, J. E. Moser, M. Grätzel and N. G. Park, *Sci. Rep.*, 2012, **2**, 00591.
- 4 B. Julian, P. Norman, M. Soo-Jin, H. B. Robin, G. Peng, M. K. Nazeeruddin and G. T. Michael, *Nature*, 2013, **499**, 316–319.
- 5 H. Zhou, Q. Chen, G. Li, S. Luo, T. B. Song, H. S. Duan, Z. Hong, J. You, Y. Liu and Y. Yang, *Science*, 2014, **345**, 542–546.
- 6 W. S. Yang, J. H. Noh, N. J. Jeon, Y. C. Kim, S. Ryu, J. Seo and S. I. Seok, *Science*, 2015, **348**, 1234–1237.
- 7 S. D. Stranks, G. E. Eperon, G. Giulia, M. Christopher, M. J. P. Alcoser, T. Leijtens, L. M. Herz, A. Petrozza and H. J. Snaith, *Science*, 2013, **342**, 341–344.
- 8 G. Xing, N. Mathews, S. Sun, S. S. Lim, Y. M. Lam, M. Grätzel, S. Mhaisalkar and T. C. Sum, *Science*, 2013, **342**, 344–347.
- 9 M. A. Green and T. Bein, *Nat. Mater.*, 2015, **14**, 559–561.
- 10 K. Leo, *Nat. Nanotechnol.*, 2015, **10**, 574–575.
- 11 H. L. Hsu, C. C. Chang, C. P. Chen, B. H. Jiang, R. J. Jeng and C. H. Cheng, *J. Mater. Chem. A*, 2015, **3**, 9271–9277.
- 12 G. Niu, X. Guo and L. Wang, *J. Mater. Chem. A*, 2015, **3**, 8970–8980.
- 13 I. Deretzis, A. Alberti, G. Pellegrino, E. Smecca, F. Giannazzo, N. Sakai, T. Miyasaka and A. L. Magna, *Appl. Phys. Lett.*, 2015, **106**, 131904.
- 14 R. K. Misra, S. Aharon, B. Li, D. Mogilyansky, I. Visoly-Fisher, L. Etgar and E. A. Katz, *J. Phys. Chem. Lett.*, 2015, **6**, 326–330.
- 15 T. Leijtens, G. E. Eperon, S. Pathak, A. Abate, M. M. Lee and H. J. Snaith, *Nat. Commun.*, 2013, **4**, 2885.
- 16 S. Ito, S. Tanaka, K. Manabe and H. Nishino, *J. Phys. Chem. C*, 2014, **118**, 16995–17000.
- 17 I. Seigo, T. Soichiro, V. Henri, N. Hitoshi, M. Kyohei and L. Peter, *ChemPhysChem*, 2014, **15**, 1194–1200.
- 18 N. Chander, A. F. Khan, P. S. Chandrasekhar, E. Thouti, S. K. Swami, V. Dutta and V. K. Komarala, *Appl. Phys. Lett.*, 2014, **105**, 033904–033905.
- 19 P. Cui, P. Fu, D. Wei, M. Li, D. Song, X. Yue, Y. Li, Z. Zhang, Y. Li and J. M. Mbengue, *RSC Adv.*, 2015, **5**, 75622.
- 20 D. Song, P. Cui, T. Wang, D. Wei, M. Li, F. Cao, X. Yue, P. Fu, Y. Li, Y. He, B. Jiang and M. Trevor, *J. Phys. Chem. C*, 2015, **119**, 22812–22819.
- 21 Z. Zhang, D. Wei, B. Xie, X. Yue, M. Li, D. Song and Y. Li, *Sol. Energy*, 2015, **122**, 97–103.
- 22 H. H. Jin, H. J. Han, D. Kim, T. K. Ahn and H. I. Sang, *Energy Environ. Sci.*, 2015, **8**, 1602–1608.
- 23 J. A. Christians, P. A. M. Herrera and P. V. Kamat, *J. Am. Chem. Soc.*, 2015, **137**, 1530–1538.
- 24 D. Song, P. Cui, X. Zhao, M. Li, L. Chu, T. Wang and B. Jiang, *Nanoscale*, 2015, **7**, 5712–5718.
- 25 D. Song, M. Li, Y. Li, X. Zhao, B. Jiang and Y. Jiang, *ACS Appl. Mater. Interfaces*, 2014, **6**, 7126–7132.
- 26 W. H. Nguyen, C. D. Bailie, E. L. Unger and M. D. McGehee, *J. Am. Chem. Soc.*, 2014, **136**, 10996–11001.
- 27 Q. Wang, Y. Luo and H. Aziz, *Appl. Phys. Lett.*, 2010, **97**, 063309.
- 28 Q. Wang, G. Williams, T. Tsui and H. Aziz, *J. Appl. Phys.*, 2012, **112**, 064502–064507.
- 29 Y. Liu, Y. Sun and A. Rockett, *Sol. Energy Mater. Sol. Cells*, 2012, **98**, 124–128.
- 30 S. Kuan, C. Jingjing, I. Furkan Halis, L. Pengcheng and O. Jianyong, *Nanoscale*, 2014, **7**, 896–900.
- 31 J. Cao, J. Yin, S. Yuan, Y. Zhao, J. Li and N. Zheng, *Nanoscale*, 2015, **7**, 9443–9447.